

Electronic Supporting Information (ESI)

Carboxylic and *O*-acetyl moieties are essential for the immunostimulatory activity of glucuronoxylomannan: a novel TLR4 specific immunostimulator from *Auricularia auricula-judae*

Namal Perera^{a, b, d, e, l}, Feng-Ling Yang^{a, l}, Jeffy Chern^{a, b, j}, Hsiao-Wen Chiu^{g, h}, Chih-Yu Hsieh^h, Lan-Hui Li^f, Yan-Long Zhang^{c, *}, Kuo-Feng Hua^{h, i, *}, Shih-Hsiung Wu^{a, b, j, *}

- a. Institute of Biological Chemistry, Academia Sinica, Taipei, Taiwan
- b. Chemical Biology and Molecular Biophysics Program, Taiwan International Graduate Program, Academia Sinica, Taipei, Taiwan
- c. Key Laboratory of Molecular Biology of Heilongjiang Province, College of Life Sciences, Heilongjiang University, Harbin 150080, China
- d. Department of Chemistry, National Tsing-Hua University, Hsinchu, Taiwan
- e. Faculty of Applied Sciences, Sabaragamuwa University of Sri Lanka, Sri Lanka
- f. Department of Laboratory Medicine, Linsen, Chinese Medicine and Kunming Branch, Taipei City Hospital, Taipei, Taiwan
- g. Graduate Institute of Life Sciences, National Defense Medical Center, Taipei, Taiwan
- h. Department of Biotechnology and Animal Science, National Ilan University, Ilan, Taiwan
- i. Department of Pathology, Tri-Service General Hospital, National Defense Medical Center, Taipei, Taiwan
- j. Department of Chemistry and Institute of Biochemical Sciences, National Taiwan University, Taiwan

* Corresponding authors l: equal contribution

Contents of supporting information

Content		Page
Experimental procedure		S3-S10
Figure S1	GC/MS chromatogram of partially methylated alditol acetates (PMAA) of AAPS under alkaline condition	S11
Figure S2	GC/MS chromatogram of partially methylated alditol acetates (PMAA) of reduced AAPS under non-alkaline condition	S12
Figure S3	The full view of ^1H NMR (500 MHz) spectrum of native AAPS	S13
Figure S4	The full view of ^1H NMR (500 MHz) spectrum of deacetylated AAPS	S14
Figure S5	The full view of ^1H NMR (500 MHz) spectrum of reduced AAPS	S15
Figure S6	The full view of ^{13}C NMR (500 MHz) spectrum of deacetylated AAPS	S16
Figure S7	The expanded view of ^{13}C NMR (500 MHz) spectrum of deacetylated AAPS	S17
Figure S8	The full view of ^{13}C DEPT- NMR (500 MHz) spectrum of deacetylated AAPS	S18
Figure S9	1D selective TOCSY spectra of AAPS (500 MHz, D_2O) to identify ring protons of β -xylose (A) and β -glucuronic acid (B)	S19
Figure S10	2D COSY (800 MHz, D_2O) spectrum of deacetylated AAPS at 340 K	S20
Figure S11	Anomeric region of NOESY (800 MHz) spectrum of deacetylated AAPS	S21
Figure S12	The full view of NOESY (800 MHz) spectrum of deacetylated AAPS	S22
Figure S13	Anomeric region of HSQC (800 MHz) spectrum of deacetylated AAPS	S23
Figure S14	The ring proton region of HSQC (800 MHz) spectrum of deacetylated AAPS	S24
Figure S15	The full view of HSQC (800 MHz) spectrum of deacetylated AAPS	S25
Figure S16	Anomeric region of HMBC (500 MHz) spectrum of deacetylated AAPS	S26
Figure S17	The full view of HMBC (500 MHz) spectrum of deacetylated AAPS	S27
Figure S18	GC/MS chromatogram of partially methylated alditol acetates (PMAA) of native AAPS under non-alkaline condition	S28
Figure S19	Native AAPS is endotoxin free	S29
Figure S20	Competition assays using TLR4-MD2 neutralizing antibody.	S30
Figure S22	Effect of lipid IVa on AAPS-activated human THP-1 macrophages.	S31
Table S1	GC/MS data table of native AAPS under alkaline condition	S32
Table S2	GC/MS data table of reduced AAPS under non-alkaline condition	S33
Table S3	The ^1H and ^{13}C -NMR chemical shift data table of deacetylated AAPS	S34
Table S4	GC/MS data table of native AAPS under non-alkaline condition	S35
Table S5	Hydrogen bonds between AAPS and the corresponding residue in dimeric TLR4/MD-2 complexes	S36

Materials and Methods

Extraction of polysaccharides

Finely powdered mushroom samples (20 g) were extracted with absolute ethanol (100 ml) at room temperature to remove ethanol soluble small organic molecules. Residue was dried at 70 °C, for 30 minutes to remove residual ethanol. Completely dried residue (5 g) was extracted with 200 mL of deionized water, at 4 °C overnight, to obtain cold water soluble polysaccharides. Resulting extract was then centrifuged at 4000 g for 20 minutes and supernatants were filtered, ethanol precipitated and lyophilized. To remove nucleic acids and proteins, each extract was subjected to nuclease and protease enzyme digestion. Briefly, 50 mg of lyophilized extract was dissolved in 10 mL of 20 mM Tris-HCl buffer (pH 8 with Ca^{2+} and Mg^{2+} 5 mM each), treated with 0.1 mg of DNase and RNase (Roche) and incubated at 37 °C overnight. After overnight incubation, extracts were treated with 0.3 mg of Proteinase K (Genaxis) and incubated at 37 °C overnight. Enzymes were deactivated by boiling the samples at 100 °C for 10 minutes, centrifuged (4000 g, 20 minutes, 4 °C) and supernatants were dialyzed against distilled water using 8-10 kDa cellulose membrane for 48-72 h by changing distilled water at every 24 h. Dialyzed samples were lyophilized and stored at -20 °C.

Extracted polysaccharides (10-20 mg) was purified by gel filtration chromatography (Toyopearl HW65F; Tosoh biosciences, Tokyo, Japan; column dimensions: H × D, 95 cm x 1.6 cm) using water containing 0.02% NaN_3) as the eluent with a flow rate of 0.4 mL/min. Eighty fractions (3 mL/each) were collected. Presence of polysaccharides in each fraction was spectrometrically detected at 490 nm with phenol-sulfuric acid reagent. Under the same conditions, dextran standards of 500, 70 and 10 kDa were used as internal standards to calibrate the column. Separated fractions were dialyzed against distilled water using 8-10 kDa cellulose membrane for 48-72 h by changing distilled water at every 24 h. Dialyzed samples were lyophilized and further purified by ion exchange chromatography using a Mono Q 5/50 GL anion exchange column (I.D.×H, 5 mm x 50 mm) attached to AKTA FPLC system. The column was pre-equilibrated with the 0.1 M NaCl in 20 mM Tris-HCl buffer (pH 7.2) containing 0.02% NaN_3 . Samples were eluted with a 0.1 M to 1 M NaCl gradient in 20 mM Tris buffer (pH 7.2) at the flow rate of 0.5 mL/min. Forty fractions (1 mL/each) were collected and the presence of polysaccharides in each fraction was detected at 490 nm with phenol-sulfuric acid reagent. Protein contents of polysaccharide

samples were determined by Bradford's method. Bovine serum albumin was used as the protein standard.

Monosaccharide analysis

The monosaccharide composition was determined by acidic hydrolysis with 0.5 M methanolic HCl (Supelco) at 80 °C for 16 h, N-acetylation with pyridine/acetic anhydride and methanol (10, 50 and 500 µL respectively) and trimethylsilylated with Sylon HTP (HMDS/TMCS/pyridine, 3:1:9) trimethylsilylating reagent (Supelco). The final trimethylsilylated products were dissolved in n-hexane and analyzed by Bruker SCION GC-MS system (Agilent J&W HP-5ms, GC column, ID 0.25 mm, length 30 m, film thickness: 1.00 µm).

Direct determination of uronic acid content by spectrophotometry

Uronic acid contents of polysaccharide fractions were determined by the method described by Filisetti-Cozzi and Carpita¹. Briefly the polysaccharide samples were dissolved in 200 µL of deionized water, and 1200 µL of 12.5 M sodium tetraborate in concentrated H₂SO₄ was added. After vigorous vortexing, the mixture was boiled for 5 minutes, cooled to room temperature, and 20 µL of 0.15% 3-hydroxydiphenol (Sigma–Aldrich) was added. Absorbance was measured at 520 nm. Glucuronic acid was used as the standard.

Reduction of uronic acid residues

Uronic acid residues were reduced as described by Taylor et al². Briefly, 35 mg of purified polysaccharide was dissolved in 5 mL of deionised water and carboxylic acid groups were activated by adding 350 mg of 1-cyclohexyl-3-(2-morpholinoethyl)carbodiimide metho-*p*-toluenesulfonate (CMC). The pH was maintained at 4.75 (with 0.1 M HCl) for 1 h at room temperature. The resulting solution was treated with 2 M NaBH₄ (drop wise addition over 1 h), maintaining the pH at 7 (with 2 M HCl). The final product was dialyzed (1 kDa cellulose membrane) against deionized water for 72 h, changing water at every 12 h and freeze-dried. Resulting carboxyl-reduced polysaccharide was further fractionated and purified by gel filtration and ion exchange chromatography.

Linkage analysis (Hakomori methylation)³

Polysaccharides samples (0.5-1 mg) were permethylated with CH₃I/ dimethyl sulfoxide (DMSO) under alkaline condition hydrolyzed by 2M TFA at 120 °C for 2 h and reduced by NaBD₄ in ethanol for 2 h at room temperature. The excess NaBD₄ was destroyed by adding few drops of glacial acetic acid and co-evaporated with methanol. The residue was acetylated with pyridine/acetic anhydride (1:1, v/v) at 80 °C for 1 h. Acetylated product was extracted into chloroform and the solvent was evaporated with a stream of N₂ gas. Resulting PMAA derivatives were dissolved in hexane and analyzed by GC-MS.

Determination of *O*-acetylation level and *O*-acetylation positions of native polysaccharide

O-acetylation rate was measured as described by Hestrin⁴. Glucose pentaacetate was used as the standard to establish the calibration plot. Positions of *O*-acetylation were determined by the methylation method described by Peter Prehm⁵. Briefly 5 mg of purified polysaccharide was suspended in trimethylphosphate (1 mL), by sonication and treated with 2, 6-Di-tert-butylpyridine (150 µL) and methyl trifluoromethanesulfonate (100 µL) and allowed to react for 2 h at 50 °C. The resulting solution was then distributed between chloroform (5 mL) and water (20 mL). Separated chloroform layer was concentrated and passed through an LH-20 column (H x D; 20 cm x 1.5 cm) using methanol/chloroform (1:1) as the eluting solvent. Recovered methylated polysaccharides were analyzed by conventional linkage analysis protocol.

Deacetylation

A portion of crude polysaccharides (100 mg) was chemically de-*O*-acetylated by incubation with 0.1 M NaOH for 4 h at 37 °C. The resulting de-*O*-acetylated polysaccharide was dialyzed, lyophilized and further purified by gel filtration (Toyopearl HW65F; Tosoh biosciences, Tokyo, Japan; column dimensions: H x D, 95 cm x 1.6 cm) and anion exchange (DEAE, 0.1 M to 1 M NaCl gradient) chromatography respectively.

Preparation of AAPS with varying amounts of acetyl contents

Native AAPS samples (10 mg each) were treated with different concentrations of NaOH solutions (0.0001 M to 0.1 M) at 37 °C for 30 min, neutralized with diluted acetic acid, dialyzed and lyophilized. *O*-acetyl content of each sample was measured as described by Hestrin⁴.

Nuclear Magnetic Resonance (NMR) Spectroscopy

The polysaccharide of *Auricularia auricula-judae* in D₂O (20 mg/mL) were analyzed by NMR using AVANCE 500 and 800 MHz spectrometer at 340 K. Chemical shifts are referenced to the residual signal for D₂O at δ 4.7 ppm (¹H). One-dimensional (1D)/two-dimensional (2D)-NMR were carried out with standard pulse sequence provided by Bruker. 2D total correlation spectroscopy (TOCSY) experiments were recorded with mixing times of 80 and 120 ms. Two-dimensional correlation spectroscopy (2D-COSY) was used to assign the proton chemical shifts of H1-H6 of the mannose and galactose. The heteronuclear single-quantum coherence (HSQC) spectrum was recorded with PL-120dB to observe the coupling constants of anomeric positions. In addition, NOESY (800 MHz, delay time 400 ms) and HMBC (500 MHz) was recorded to assign the linkages of polysaccharide.

Cell Culture

The Raw 264.7 murine macrophage cell line was obtained from American Type Culture Collection (Rockville, MD). Seven-to-nine-week-old male C57BL/6JNal mice were purchased from the National Laboratory Animal Center (Taipei, Taiwan). Mice experiments were performed with the approval of the Institutional Animal Care and Use Committee of the National Ilan University (approval number: 106-13) and in accordance with the NIH Guide for the Care and Use of Laboratory Animals. For the preparation of mice bone marrow-derived macrophages, marrow was collected from C57BL/6JNal mice femur and tibia and incubated for 7 days in culture medium containing M-CSF (Pepro Tech, London, UK).

Macrophage activation - nitric oxide (NO) assay

Raw 264.7 murine macrophage cell line growing in RPMI medium (supplemented with 10% FBS) were seeded (1×10^5 cells/well) in 48 well cell culture plates in triplicates. Cells were left overnight for attachment and then incubated with the positive control LPS (*Escherichia coli* O127: B8; 1 μ g/mL) or polysaccharides (1-50 μ g/mL) in a humidified atmosphere of 5% CO₂, at 37 °C for 24 h. After 24 h of treatment, culture supernatant of each well was collected and NO content was determined using Griess reagent (1:1 of 0.1% 1-naphthylethylenediamine in 5% phosphoric acid and 1% sulfanilamide in 5% phosphoric acid). The standard curve was created by using known concentrations of sodium nitrite, and the absorbance was measured at 540 nm.

Cytokine Measurement

Cells (1×10^5 cells/well) were seeded in 24 well plates and treated with polysaccharides at varying concentrations (1-10 $\mu\text{g/mL}$) and incubated for 24 h at 37 °C. The levels of cytokines in culture medium (TNF- α , IL-6 or IL-1 β) were measured using ELISA (R&D Systems, Inc., Minneapolis, MN) according to the manufacturer's protocol.

Elimination of possible endotoxin contamination

To avoid the possible endotoxin contaminations during the sample preparation process, laboratory reagents and water were continuously subjected to *Limulus* Amebocyte Lysate (LAL) assay and confirmed the absence of endotoxins. Polysaccharide isolation process was conducted under conditions that minimize possible bacterial contaminations.

Polymyxin B assay and *Limulus* Amebocyte Lysate (LAL) based endotoxin assay are considered as common endotoxin detection methods. However, both methods are not specific to endotoxins and have given false positive responses in many instances⁶⁻⁸. Polymyxin B, is a cationic bacterial peptide which from strong electrostatic interactions with negatively charge molecules including LPS. In the present study we observed that polymyxin B pretreatment partially inhibited the AAPS induced NO and TNF- α production. Moreover, LAL assay showed equally positive responses for all three types polysaccharides including biologically inactive deacetylated and reduced AAPS samples. This is not surprising because polymyxin B might interact with negatively charged AAPS to inhibit NO and TNF- α production. It has been further reported that many plant polysaccharides positively interfere with LAL assay, presumably mimicking LPS^{7,8}. Since deacetylated and reduced polysaccharides are non-immunogenic, it is obvious that positive responses of LAL assay were due to the structural nature of AAPS and not because of any endotoxin contamination. Similar observations have been previously reported by several research

groups indicating the importance of further improvements in available detection methods or necessity of more specific analysis methods in the field of endotoxin research^{8,9}.

However, ammonium pyrrolidinedithiocarbamate (PDTC), an inhibitor of NF- κ B, significantly attenuated the LPS induced TNF- α production ($p < 0.01$) in raw 264.7 macrophages whereas AAPS induced TNF- α levels were not affected by PDTC even at high concentrations as 25 μ g/mL (**Figure S19**). These results therefore suggest that AAPS is endotoxin free. Activation of TLR4 stimulates the phosphorylation/activation of the ERK1/2, JNK1/2 and p38 and the activation of nuclear factor κ B (NF- κ B)-dependent gene transcription, etc. From different degrees of PDTC inhibition (NF- κ B inhibitor) result showed that LPS and AAPS might be stimulated distinct signaling pathways in macrophages, although both of them displayed some common features including TLR4 receptor and induction of some subsets of cytokines in different levels.

Further it was suggested that cell wall-dissociated LPS that are measured with the Limulus assay, whereas the GC-MS methods allow determination of total concentration of LPS, including Limulus-inactive LPS, gram-negative, and cell debris¹⁰. Detection limit of 1 ng of *E. coli* LPS per ml was reached. Therefore, we had chosen the GC-MS method to assay the existence of LPS by analyzing methyl and TMS derivatives of 3-hydroxy and 2-hydroxy fatty acids^{11,12}.

Briefly, 15 mg polysaccharide was methanolysed and lipid part was extracted into n-hexane, trimethylsilylated and analyzed by GC-MS. Me/TMS derivatives of 3-hydroxy acids, 2-hydroxy acids were specifically detected by monitoring m/z 175 and 211 respectively. Even we used high amounts of polysaccharides sample (15 mg) for acidic-methanolysis, TMS derivation method and GC-MS, there was no detected m/z values of 175, 211, to confirm the absence of 2 or 3-hydroxy fatty acid. There was no LPS existence in AAPS sample. The positive LPS control showed the m/z 175 spectrum.

Docking calculation of the mTLR4/MD-2 in complex with AAPS

Due to the essentiality of ligand-induced dimerization in TLR4 activation, the crystal structure of mouse TLR4/MD-2 (*mTLR4/MD-2*) in complex with hexaacylated Re-LPS¹³ (PDB ID: 3VQ2) was prepared for our docking calculation. Ligand (one repeating unit of AAPS) was generated by *PRODRG*¹⁴ in the minimized state. The LPS-binding site of the complex was selected and gridded using *AutoGrid 4.0*. Subsequently, AAPS was docked against target protein grid using a Lamarckian Genetic search algorithm (LGA) with default parameters by *AutoDock Vina* in *PyRx*. The best pose (-8.0 kcal/mole) was used for later MD simulation. The model of protein–ligand complex systems was further MD simulated using *NAMD 2.12*¹⁵. Briefly, the docked *mTLR4/MD-2/AAPS* complex was solvated with the flexible TIP3P water system in a periodic box (12 Å length was applied to each axis). Protein structure file (PSF) of the complex was generated by *CHARMM* force field and topology parameters of protein and AAPS (for AAPS, files were generated from *CHARMM General Force Field* (CGenFF) program) using *psfgen* in *VMD v1.9.3*¹⁶. Solvated protein–ligand systems were subjected to energy minimization for 100 ps through NVT simulations with 50,000 steps using the NAMD minimization algorithm in solvent periodic boundary conditions. The final model was checked with *3D-profile*¹⁷ and *PROCHECK*¹⁸. The structural representation was created by *PyMOL* (Schrödinger, New York, NY, USA).

References

1. T. M. C. C. Filisetti-Cozzi, and N. C. Carpita, *Anal. Biochem.* 1991; *197*, 157-62.
2. R. L. Taylor and H. E. Conrad. *Biochem.* 1972; *11*, 1383-8.
3. S. Hakomori. *J. Biochem.* 1964; *55*, 205-8.
4. S. Hestrin. *J. Biol. Chem.* 1949; *180*, 249-61.

5. P. Prehm. *Carbohydr. Res.* 1980; 78, 372-4.
6. R. Vassallo and A. H. Limper. *Chest.* 116; 583-4.
7. M. Hirano, T. Matsumoto, H. Kiyohara and H. Yamada. *Planta Med.* 1994; 60, 248-52.
8. I. A. Schepetkin, K. Kouakou, A. Yapi, L. N. Kirpotina, M. A. Jutila and M. T. Quinn. *Int. Immunopharmacol.* 2008; 8, 1455-66.
9. F. L. Yang, Y. L. Yang, P. C. Liao, J. C. Chou, K. C. Tsai, A. S. Yang, F. Sheu, T. L. Lin, P. F. Hsieh, J. T. Wang, K. F. Hua and S. H. Wu. *J. Biol. Chem.* 2011; 286, 21041-51.
10. A. Sonesson, L. Larsson, A. Schutz, L. Hagmar and T. Hallberg. *Appl. Environ. Microbiol.*, 1990; 56, 1271-8.
11. A. Sonesson, L. Larsson, G. Westerdahl and G. Odham. *J. Chromatogr.* 1987; 417, 11-25.
12. Z. Mielniczuk, E. Mielniczuk and L. Larsson. *J. Microbiol. Methods.* 1993; 17, 91-102.
13. U. Ohto, K. Fukase, K. Miyake and Shimizu, T. *Proc. Natl. Acad. Sci.* 2012; 109, 7421-6.
14. A. W. Schüttelkopf and D. M. F. VanAalten. *Acta Crystallogr. Sect. D Biol. Crystallogr.* 2004; 60, 1355-63.
15. J. C. Phillips, R. Braun, W. Wang, J. Gumbart, E. Tajkhorshid, E. Villa, C. Chipot, R. D. Skeel, L. Kalé and K. Schulten. *J. Comput. Chem.* 2005; 26, 1781-1802.
16. W. Humphrey, A. Dalke and K. Schulten. *J. Mol. Graph.* 1996; 14, 33-8.
17. R. Lüthy, J. U. Bowie and D. Eisenberg. *Nature*, 1992; 356, 83-5.
18. R. A. Laskowski, M. W. MacArthur, D. S. Moss, and J. M. Thornton. *J. Appl. Crystallogr.* 1993; 26, 283-91.

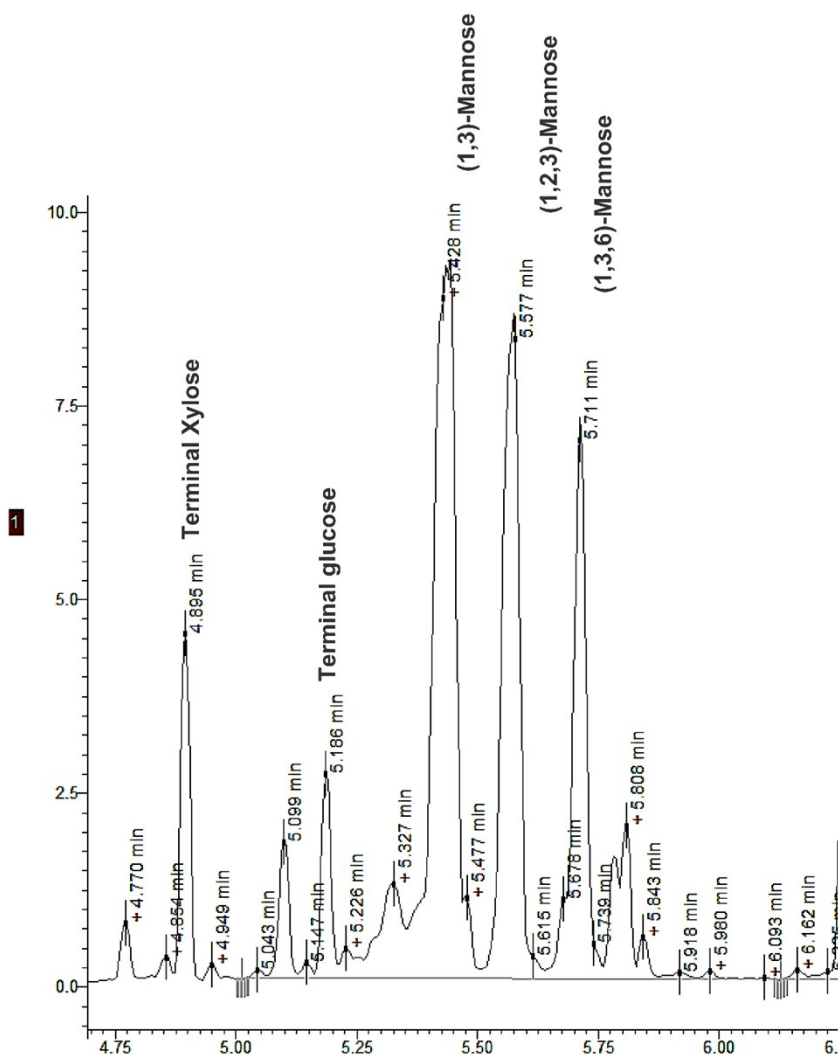


Figure S1. GC/MS chromatogram of partially methylated alditol acetates (PMAA) of AAPS under alkaline condition. Substituent acetyl groups were hydrolyzed under alkaline conditions and only glycosidic linkages could be detected

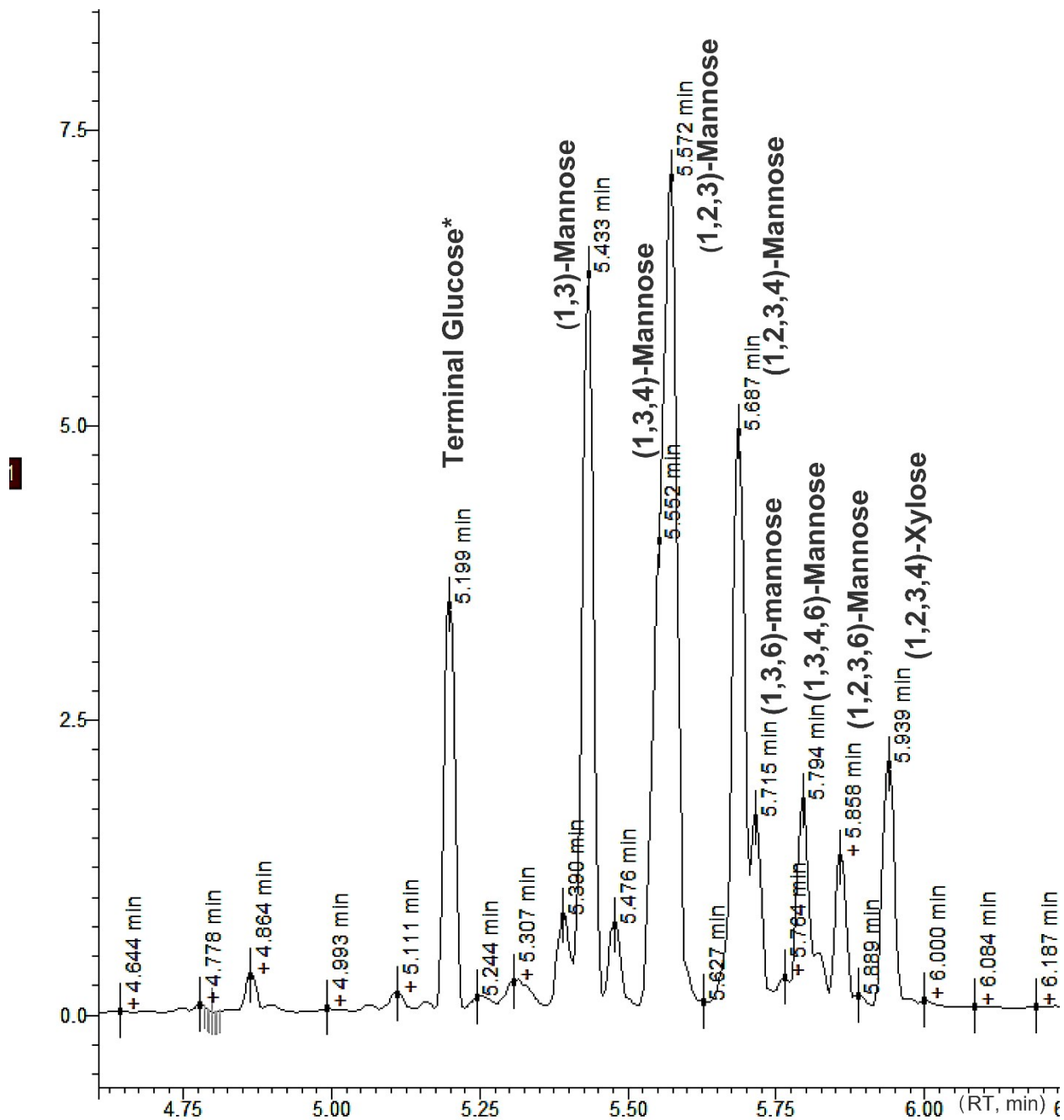


Figure S2. GC/MS chromatogram of partially methylated alditol acetates (PMAA) of reduced AAPS under non-alkaline condition. Methylation under non-alkaline condition were used to identify acetyl linkages and glycosidic linkages

Native AAPS

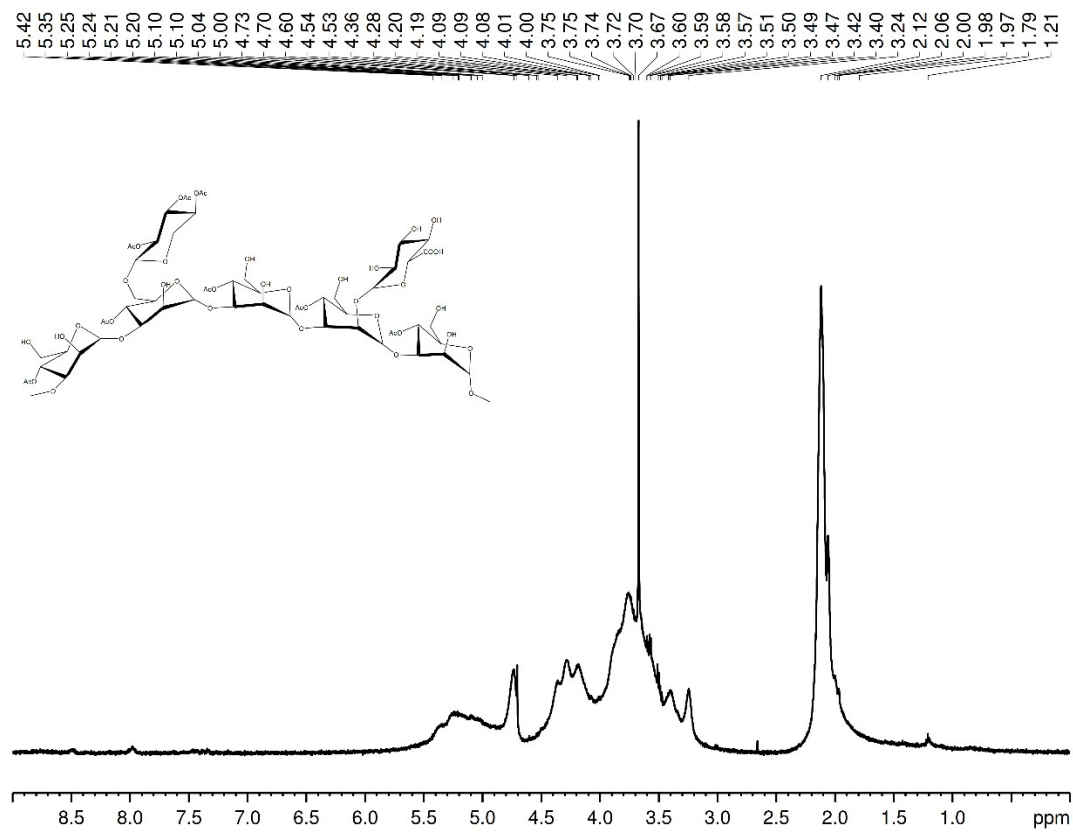


Figure S3. The full view of ^1H NMR (500 MHz, D_2O) spectrum of native AAPS at 298 K

Deacetylated AAPS

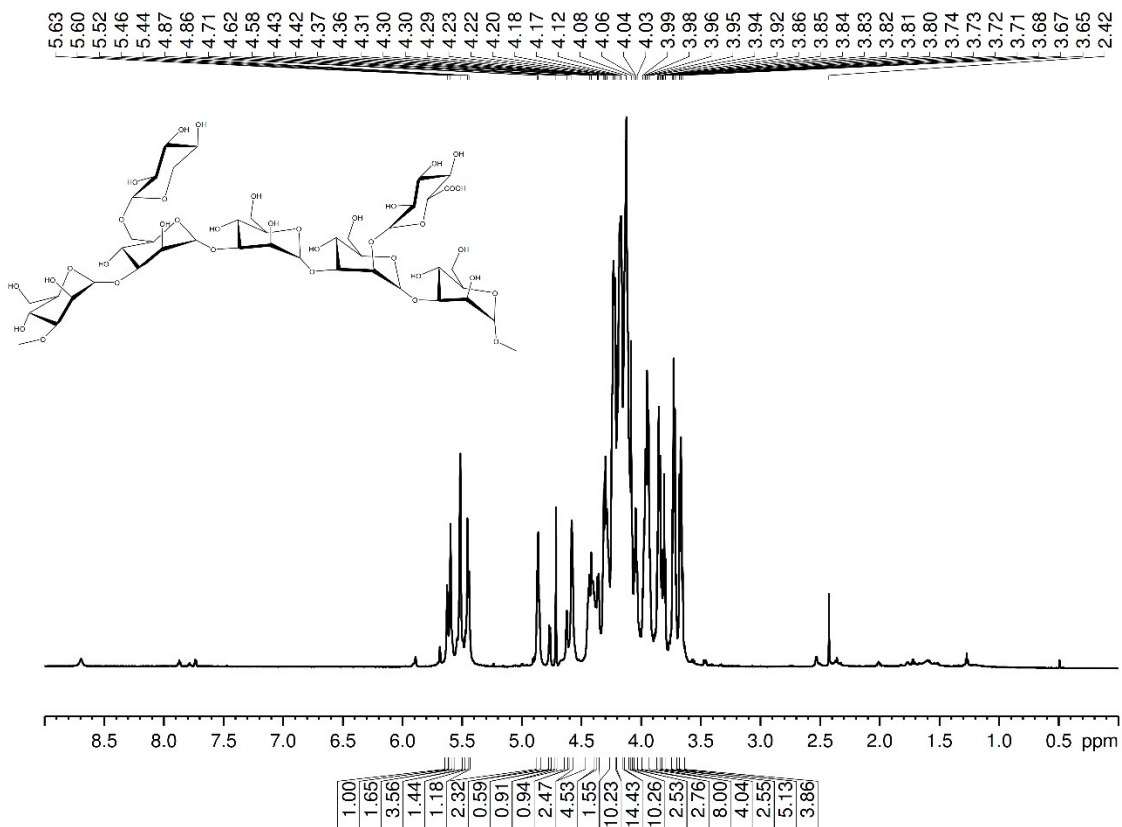


Figure S4. The full view of ^1H NMR (500 MHz, D_2O) spectrum of deacetylated AAPS at 340 K

Deacetylated AAPS

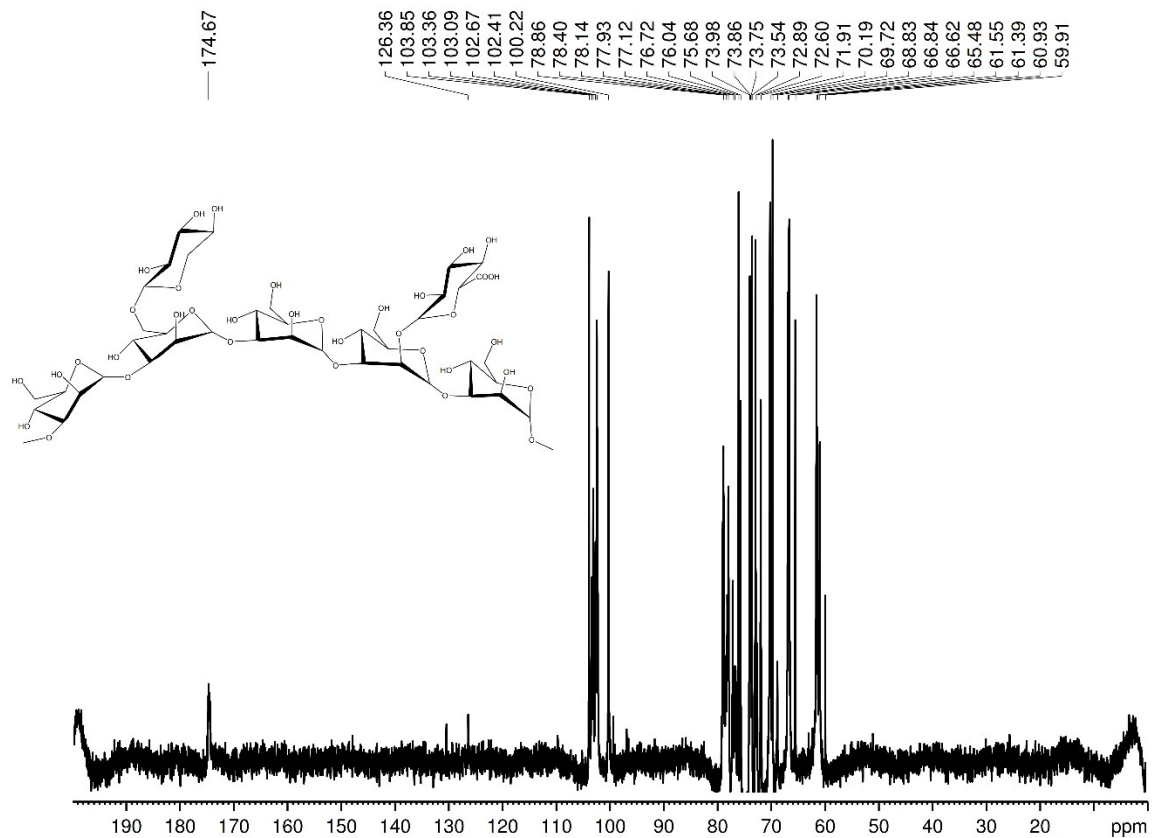


Figure S6. The full view of ¹³C NMR (500 MHz, D₂O) spectrum of deacetylated AAPS at 340 K

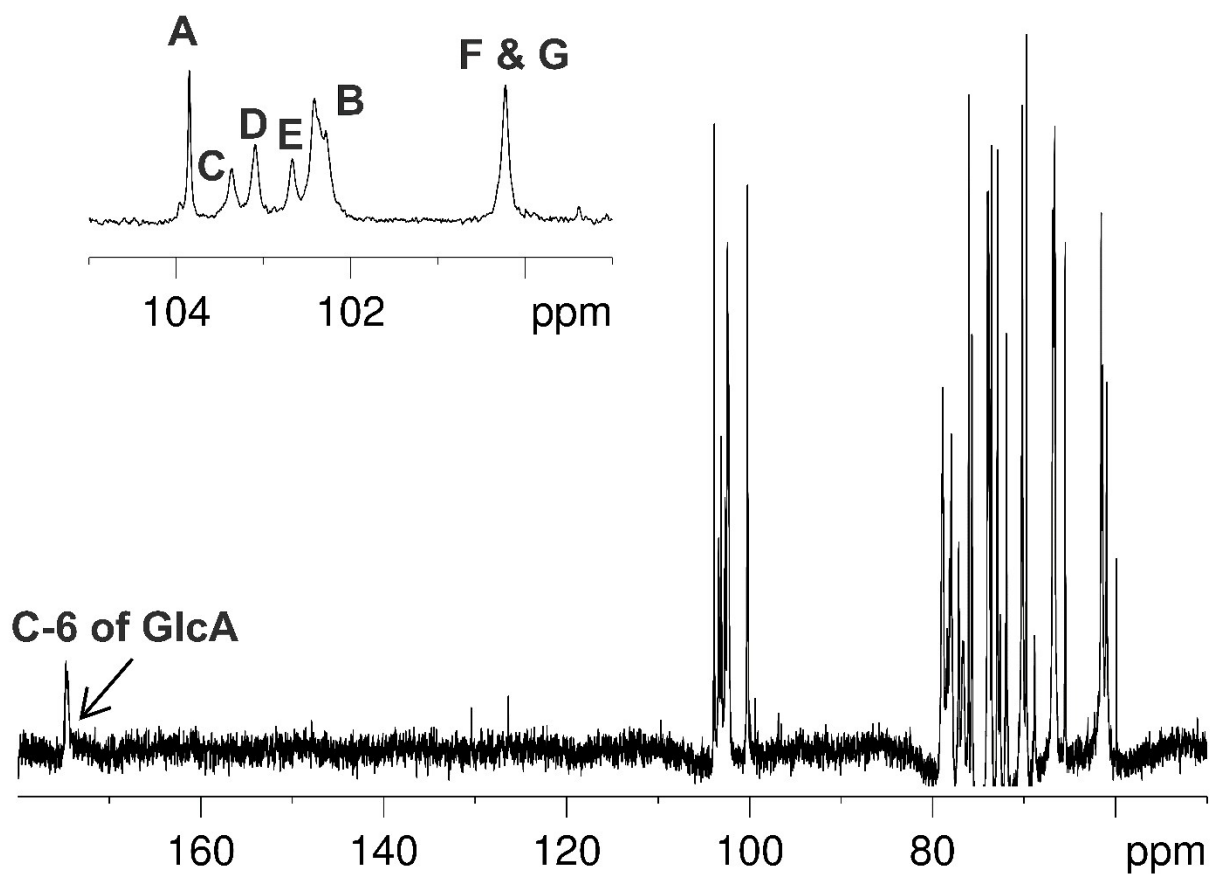


Figure S7. The expanded view of ^{13}C NMR (500 MHz, D_2O) spectrum of deacetylated AAPS at 340 K

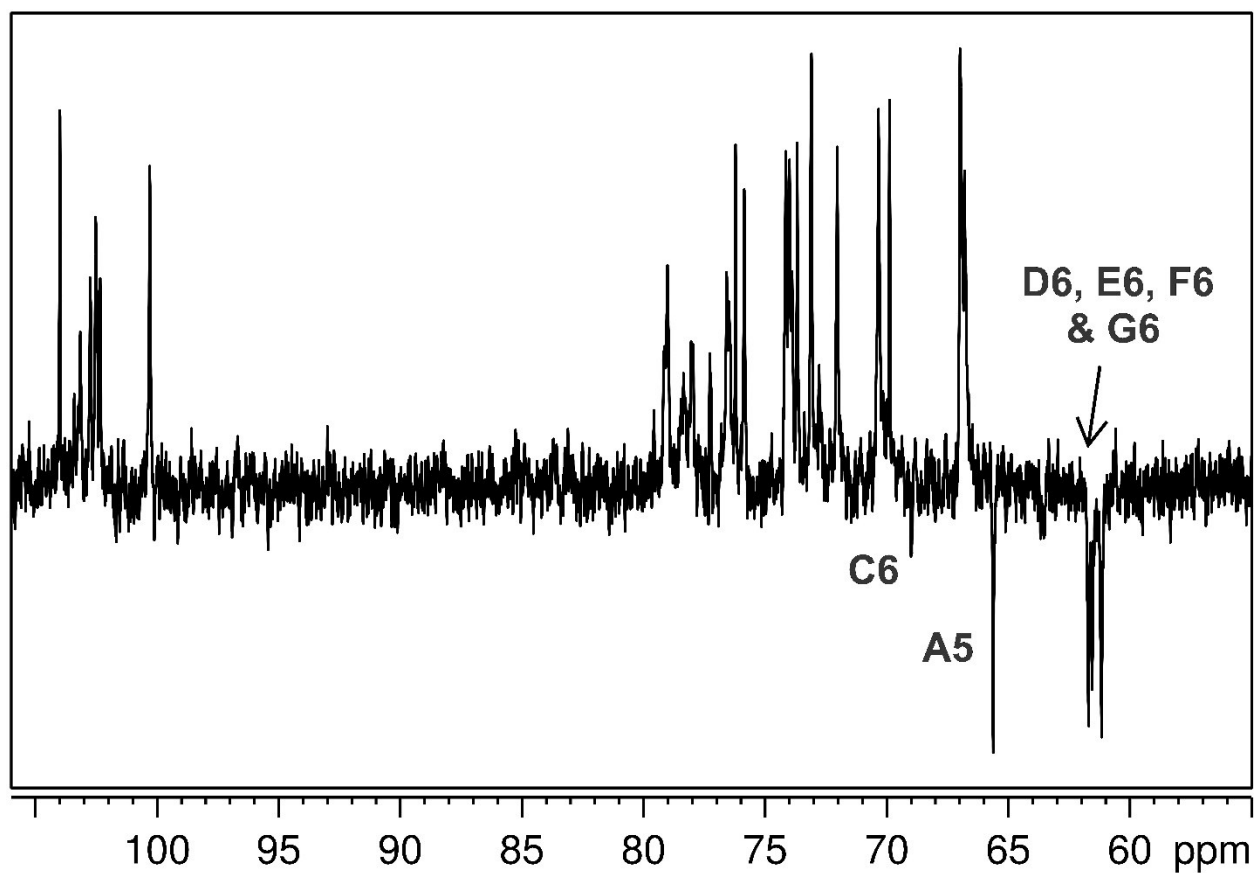


Figure S8. The full view of ^{13}C DEPT- NMR (500 MHz, D_2O) spectrum of deacetylated AAPS at 340 K

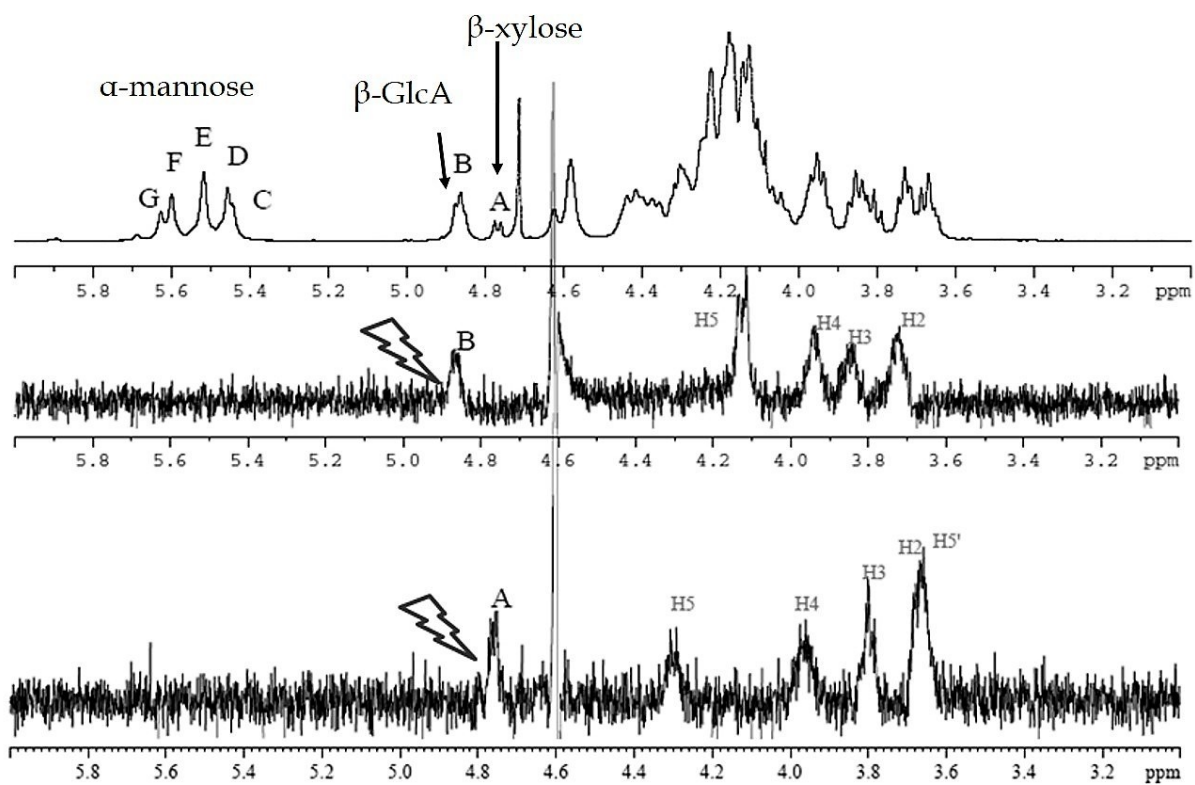


Figure S9. 1D selective TOCSY spectra of AAPS (500 MHz, D₂O) to identify ring protons of β -xylose (A) and β -glucuronic acid (B)

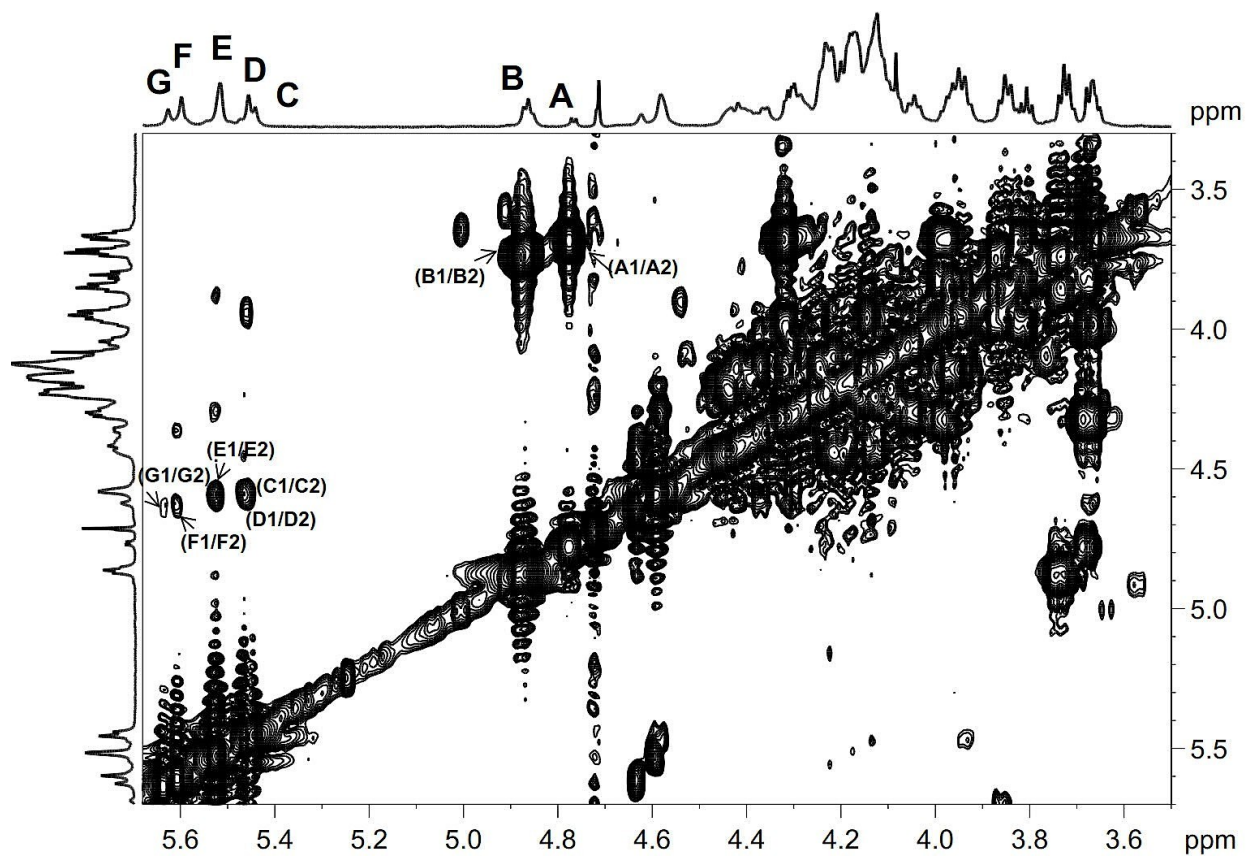


Figure S10. 2D COSY (800 MHz, D₂O) spectrum of deacetylated AAPS at 340 K. Anomeric signals were annotated. Correlations were given as H/H

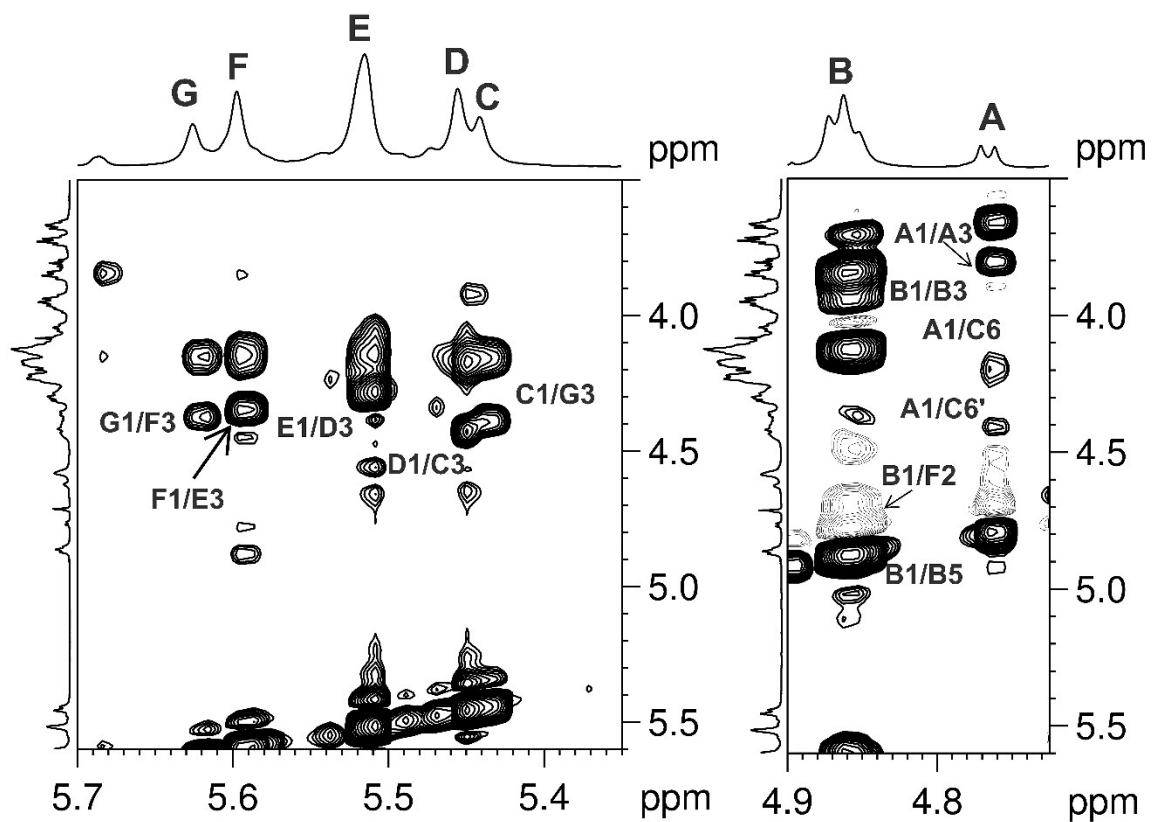


Figure S11. Anomeric region of NOESY (800 MHz, D₂O) spectrum of deacetylated AAPS at 340 K. Most relevant signals were annotated. Correlations were given as H/H

Deacetylated AAPS

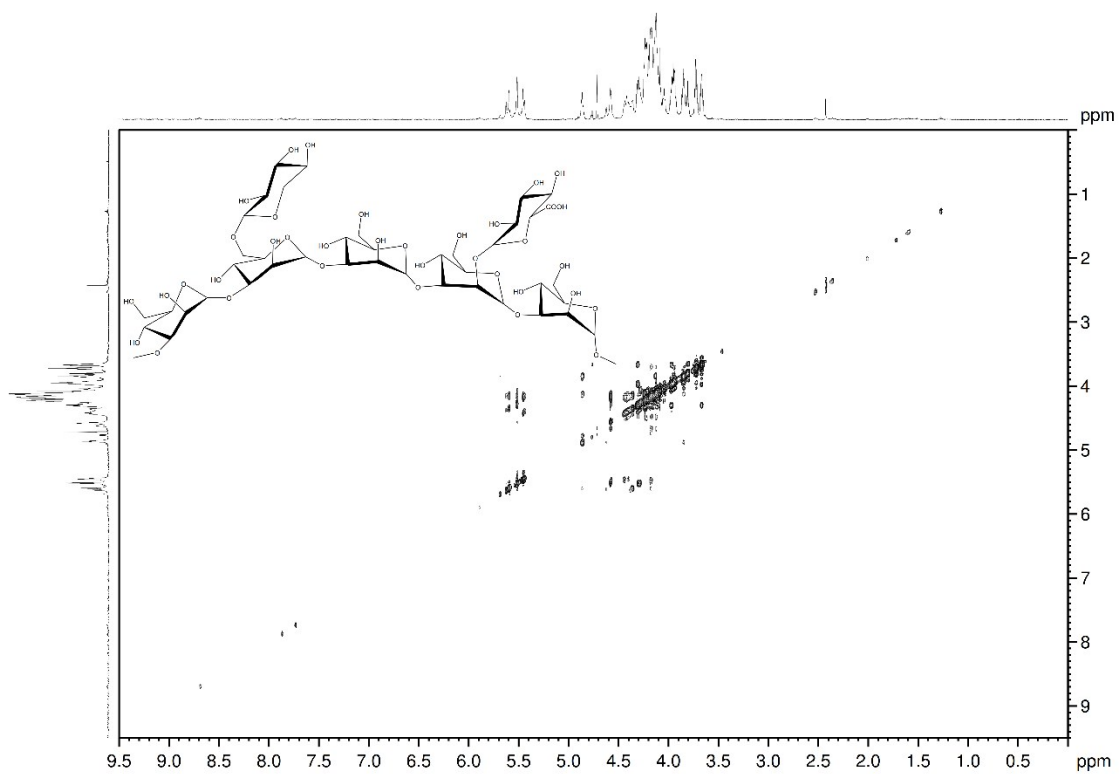


Figure S12. The full view of NOESY (800 MHz, D₂O) spectrum of deacetylated AAPS at 340 K

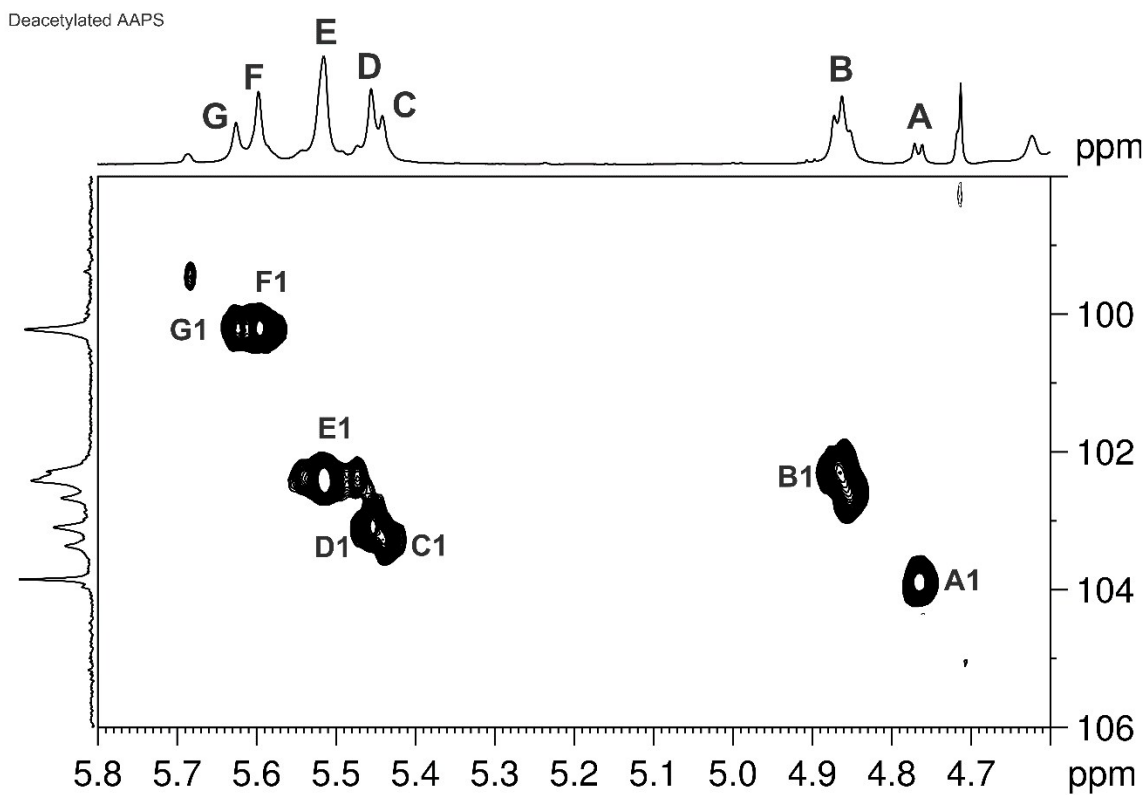


Figure S13. Anomeric region of HSQC (800 MHz, D₂O) spectrum of deacetylated AAPS at 340 K

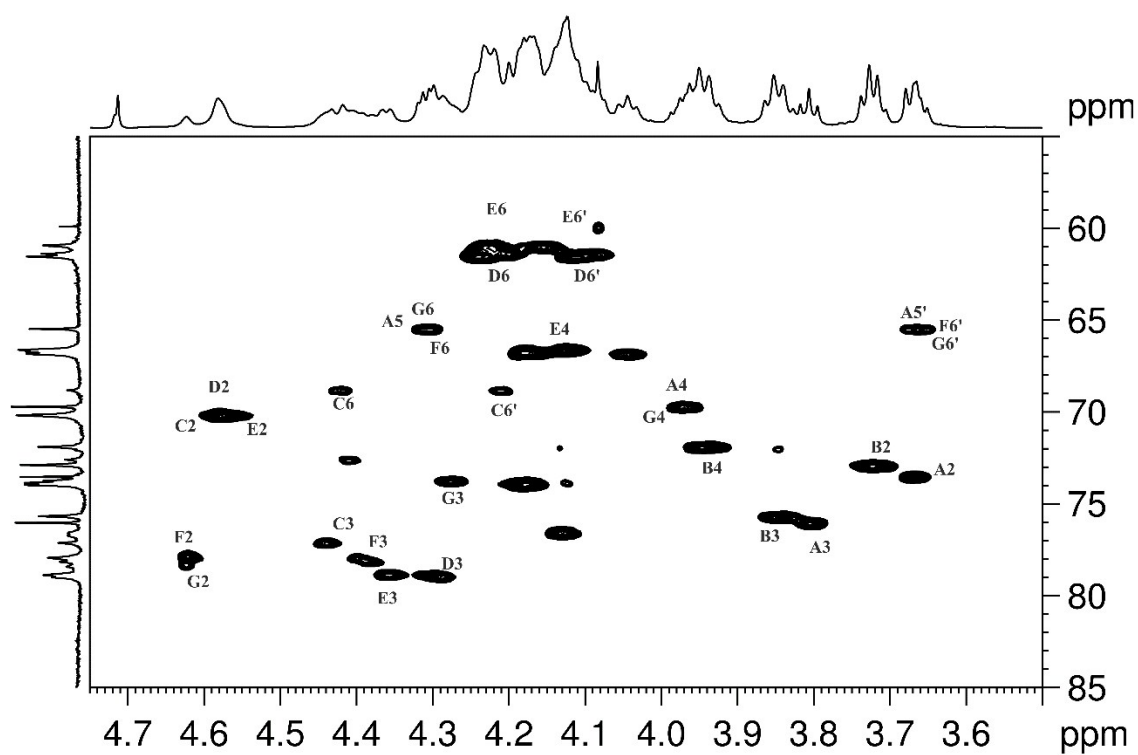


Figure S14. The ring proton region of HSQC (800 MHz, D_2O) spectrum of deacetylated AAPS at 340 K. Most relevant signals were annotated

Deacetylated AAPS

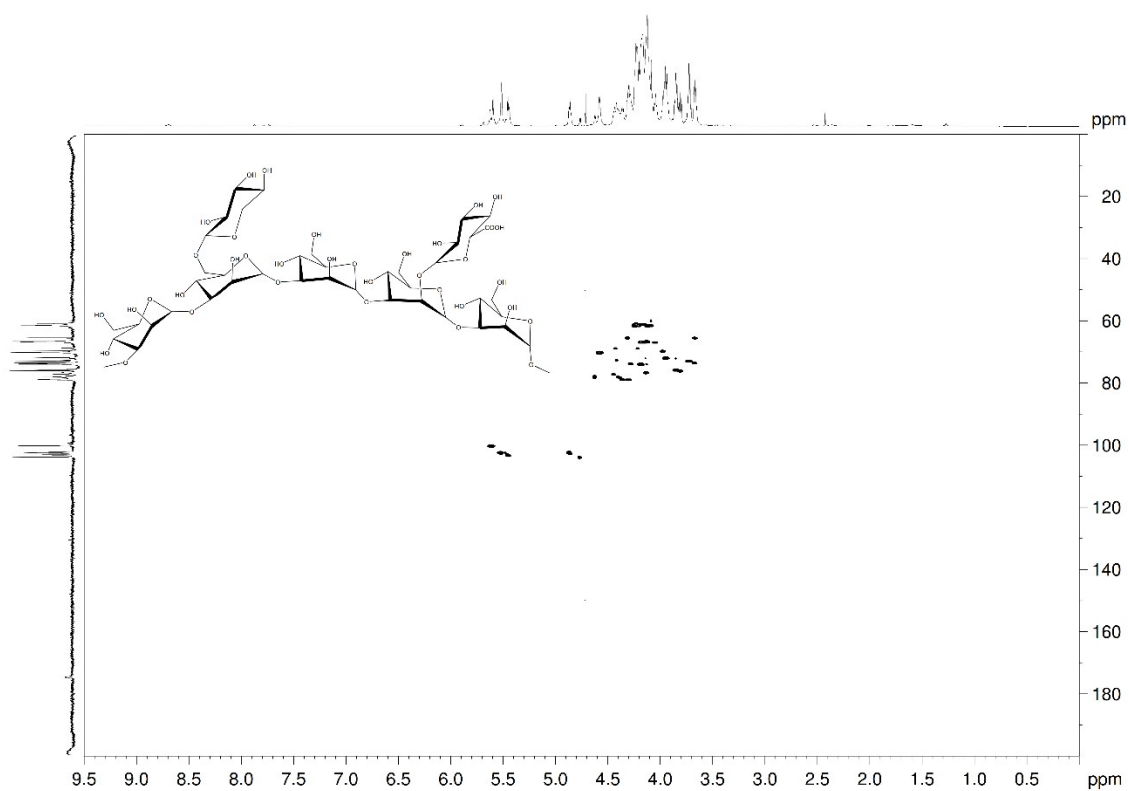


Figure S15. The full view of HSQC (800 MHz, D_2O) spectrum of deacetylated AAPS at 340 K

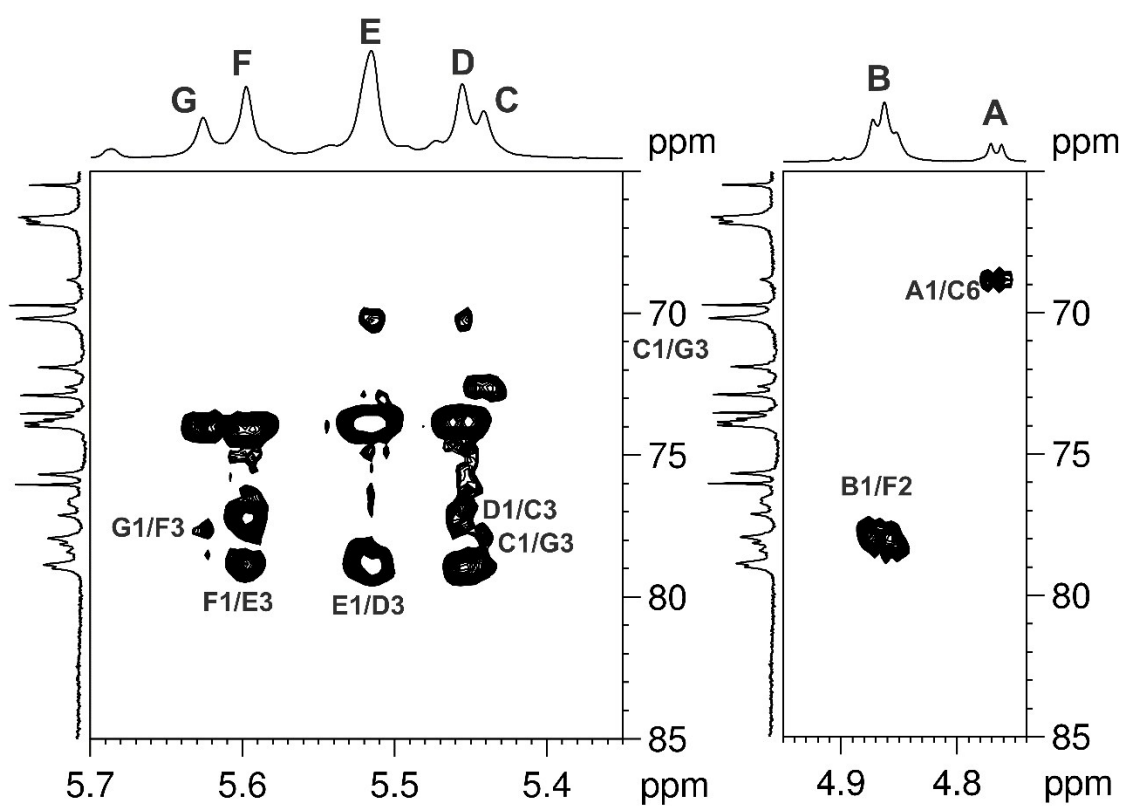


Figure S16. Anomeric region of HMBC (500 MHz, D₂O) spectrum of deacetylated AAPS at 340 K. Most relevant signals were annotated. Correlations were given as C/H

Deacetylated AAPS

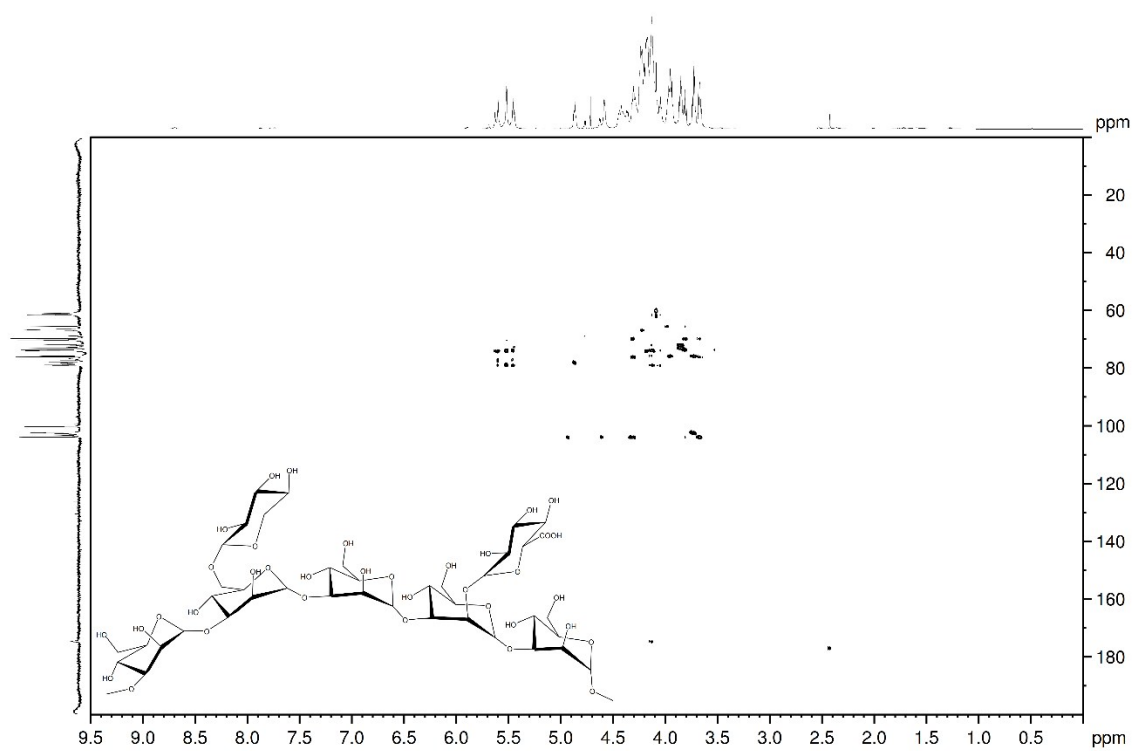


Figure S17. The full view of HMBC (500 MHz, D₂O) spectrum of deacetylated AAPS at 340 K

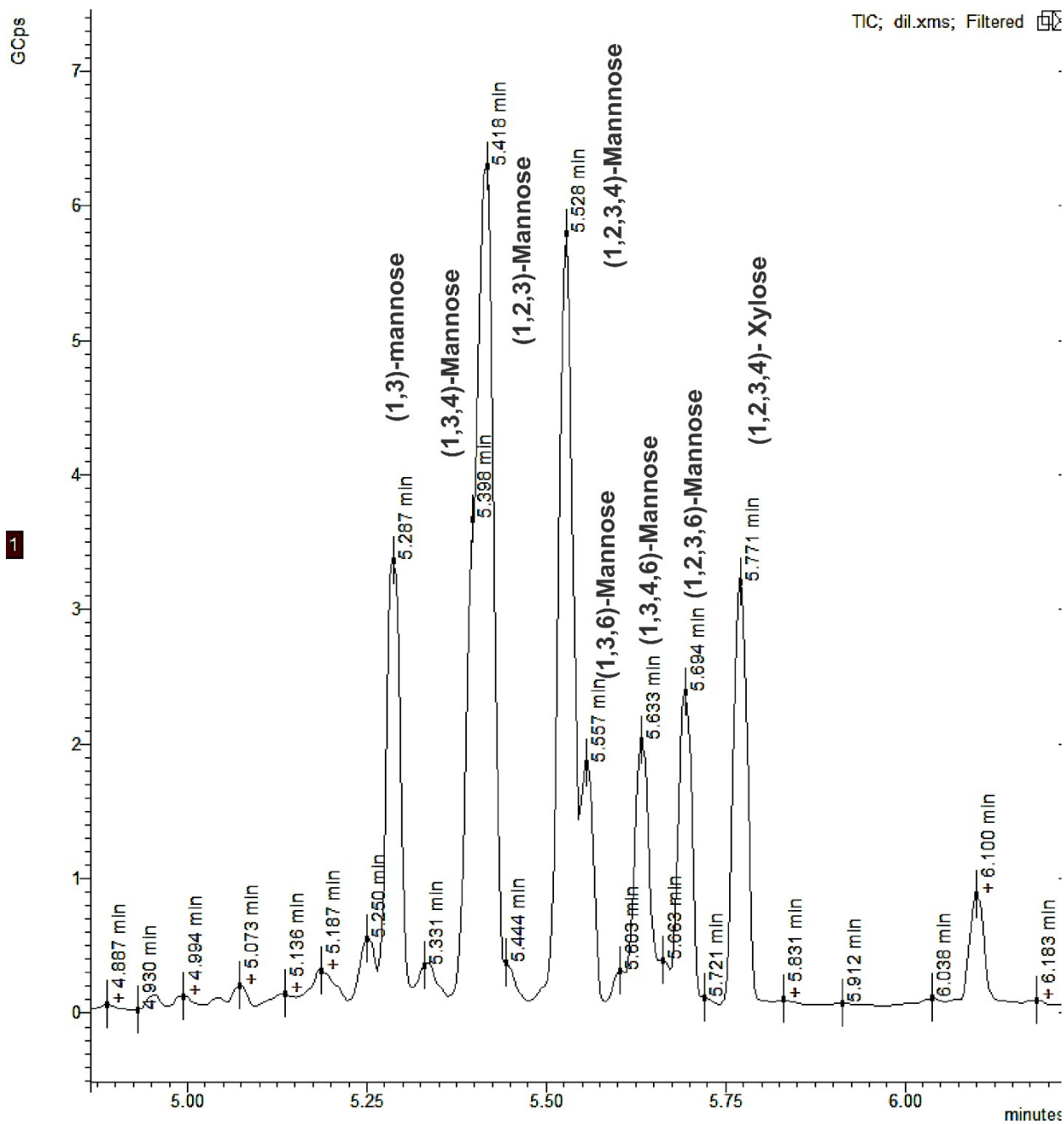


Figure S18. GC/MS chromatogram of partially methylated alditol acetates (PMAA) of native AAPS under non-alkaline condition. Methylation under non-alkaline condition were used to identify acetyl linkages and glycosidic linkages

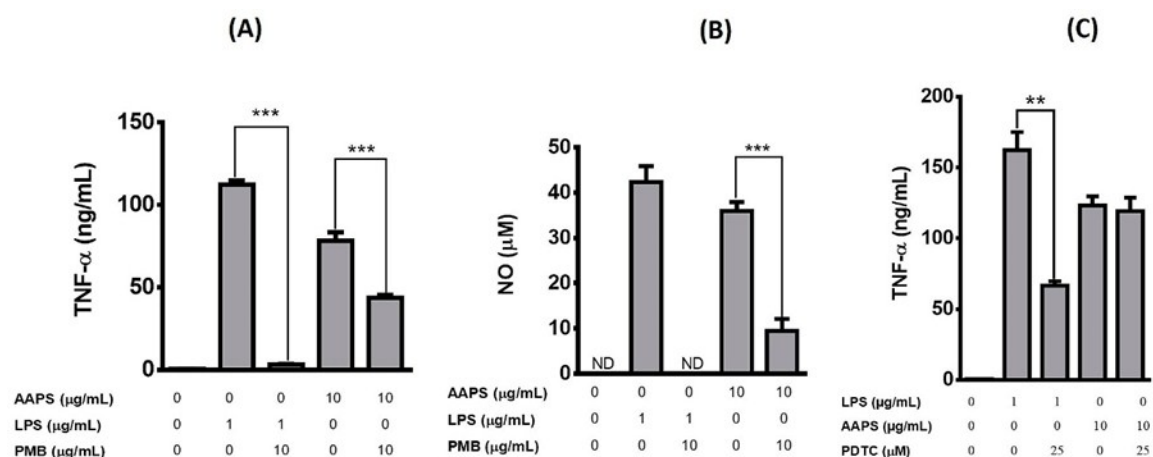


Figure S19. Native AAPS is endotoxin free

Raw 264.7 macrophages were preincubated for 30 min in the presence or absence of polymyxin B (PMB, 10 μg/mL). followed by 24 h incubation with AAPS (10 μg/mL) or LPS (1 μg/mL). The levels of TNF-α in the culture medium were measured by ELISA (A) and NO levels were measured by Griess method. (B). Raw 264.7 macrophages were preincubated for 30 min in the presence or absence of NF-κB inhibitor, (PDTC, 25 μM). followed by 24 h incubation with AAPS (10 μg/mL) or LPS (1 μg/mL). The levels of TNF-α in the culture medium were measured by ELISA (C). The results are presented as mean ±SD (n=3). ** and *** indicate significant differences at the levels of p<0.01 and p<0.001 respectively

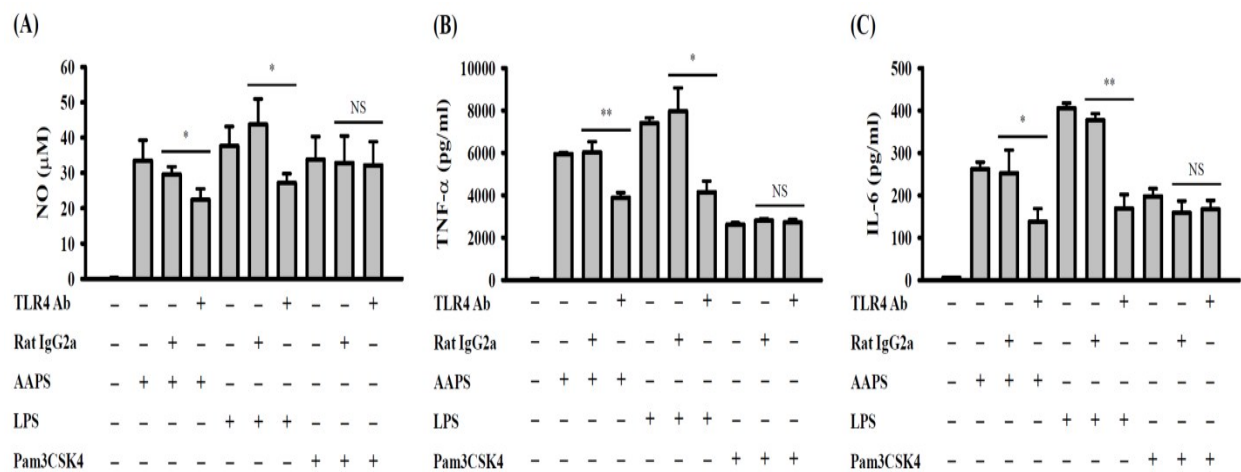


Figure S20. Effect of TLR4-MD2 neutralizing antibody on AAPS-activated mouse RAW 264.7 macrophages.

Cells (1.2×10^4 cells/well) were seeded in 96-well plates and incubated with TLR4-MD2 neutralizing antibody (30 µg/mL, Santa Cruz, # sc-13591 L) or rat IgG2a (30 µg/mL, Abcam # ab185799) for 1 h at 37 °C. The cells were then treated with AAPS (10 µg/mL), LPS (0.1 µg/mL) or Pam3CSK4 (1 µg/mL) for 6 h at 37 °C. The levels of NO (A), TNF-α (B) and IL-6 (C) in culture medium were measured using Griess reagent or ELISA according to the manufacturer's protocol. The data are expressed as the mean ± SD of three separate experiments. * and ** indicate a significant difference at the level of $p < 0.05$ and $p < 0.01$, respectively. NS: non-significant.

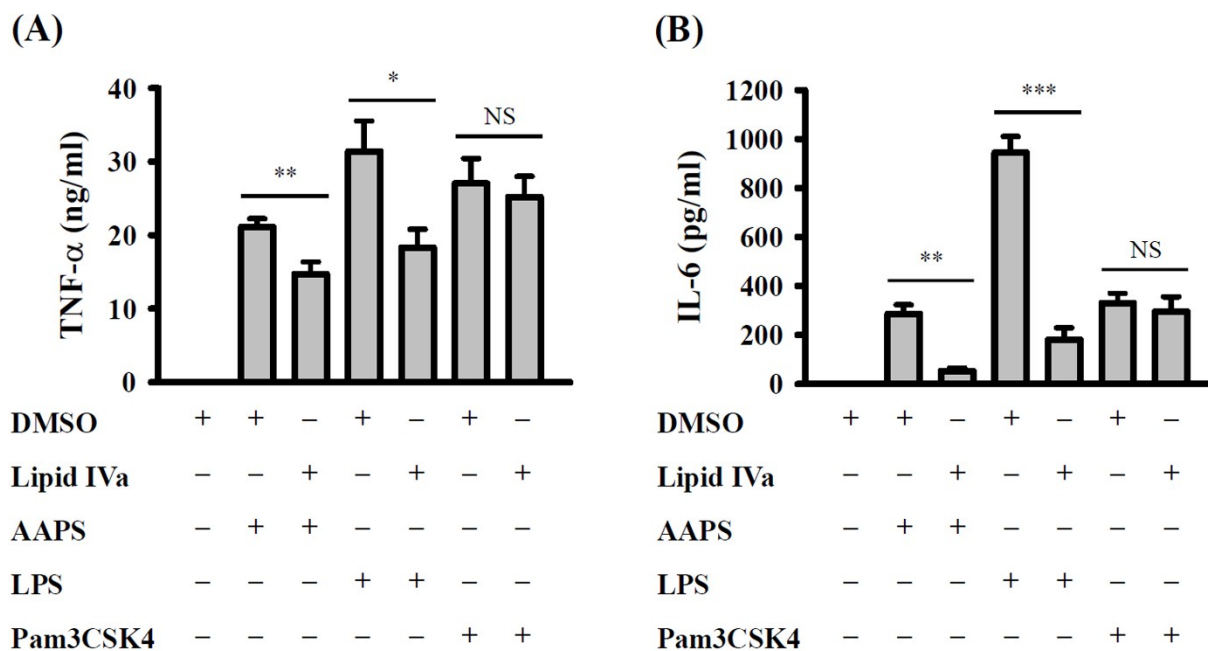


Figure S21. Effect of lipid IVa on AAPS-activated human THP-1 macrophages.

Cells (2×10^4 cells/well) were seeded in 24-well plates and incubated with lipid IVa (1 $\mu\text{g/mL}$, MyBioSource # MBS406004) or DMSO (vehicle) for 1 h at 37 $^{\circ}\text{C}$. The cells were then treated with AAPS (10 $\mu\text{g/mL}$), LPS (0.1 $\mu\text{g/mL}$) or Pam3CSK4 (1 $\mu\text{g/mL}$) for 6 h at 37 $^{\circ}\text{C}$. The levels of TNF- α and IL-6 in culture medium were measured using ELISA according to the manufacturer's protocol. The data are expressed as the mean \pm SD of three separate experiments. *, ** and *** indicate a significant difference at the level of $p < 0.05$, $p < 0.01$ and $p < 0.001$, respectively. NS: non-significant.

Retention Time (min)	Alditol derivative	MW (g/mol)	m/z	Linkage
4.89	1,5-Di- <i>O</i> -acetyl-1-deuterio-2,3,4-tri- <i>O</i> -methyl-D-xylitol	279	101, 102, 117, 118, 161, 162	Terminal
5.18	1,5-Di- <i>O</i> -acetyl-1-deuterio-2,3,4,6-tetra- <i>O</i> -methyl-D-glucitol	323	87, 102, 129, 145, 161, 162, 205	Terminal
5.43	1,3,5-Tri- <i>O</i> -acetyl-1-deuterio-2,4,6-tri- <i>O</i> -methyl-D-mannitol	351	87, 102, 118, 129, 161, 202, 234	(1,3)
5.57	1,2,3,5-Tetra- <i>O</i> -acetyl-1-deuterio-4,6-di- <i>O</i> -methyl-D-mannitol	379	87, 101, 129, 161, 202, 262	(1,2,3)
5.71	1,3,5,6-Tetra- <i>O</i> -acetyl-1-deuterio-2,4-di- <i>O</i> -methyl-D-mannitol	379	87, 101, 118, 129, 160, 189, 234	(1,3,6)

Table S1. GC/MS data table of native AAPS under alkaline condition. GC/MS spectrum was shown in figure S1

MW= theoretical molecular weight

Table S2. GC/MS data table of reduced AAPS under non-alkaline condition. GC/MS spectrum was shown in figure S2

Retention Time (min)	Alditol derivative	MW (g/mol)	m/z	Linkage
5.19	1,5-Di- <i>O</i> -acetyl-1-deuterio-2,3,4,6-tetra- <i>O</i> -methyl-D-glucitol	323	87, 102, 129, 145, 161, 162, 205	Terminal
5.43	1,3,5-Tri- <i>O</i> -acetyl-1-deuterio-2,4,6-tri- <i>O</i> -methyl-D-mannitol	351	87, 102, 118, 129, 161, 202, 234	(1,3)
5.55	1,3,4,5-Tetra- <i>O</i> -acetyl-1-deuterio-2,6-di- <i>O</i> -methyl-D-mannitol	379	87, 118, 129	(1,3,4)
5.57	1,2,3,5-Tetra- <i>O</i> -acetyl-1-deuterio-4,6-di- <i>O</i> -methyl-D-mannitol	379	87, 101, 129, 161, 202, 262	(1,2,3)
5.68	1,2,3,4,5-Penta- <i>O</i> -acetyl-1-deuterio-6- <i>O</i> -methyl-D-mannitol	407	87, 115, 129, 157, 185, 260	(1,2,3,4)
5.71	1,3,5,6-Tetra- <i>O</i> -acetyl-1-deuterio-2,4-di- <i>O</i> -methyl-D-mannitol	379	87, 101, 118, 129, 160, 189, 234	(1,3,6)
5.79	1,3,4,5,6-Penta- <i>O</i> -acetyl-1-deuterio-2- <i>O</i> -methyl-D-mannitol	351	118, 139	(1,3,4,6)
5.86	1,2,3,5,6-Penta- <i>O</i> -acetyl-1-deuterio-4- <i>O</i> -methyl-D-mannitol	351	87, 129, 189, 162	(1,2,3,6)
5.94	1,2,3,4,5-Penta- <i>O</i> -acetyl-1-deuterio-D-xylitol	363	86, 115, 128, 145, 159, 188, 218	(1,2,3,4)

MW= theoretical molecular weight

Table S3. The ^1H and ^{13}C -NMR chemical shift data table of deacetylated AAPS

Table S4. GC/MS data table of native AAPS under non-alkaline condition. GC/MS spectrum was shown in figure S18

Retention Time (min)	Alditol derivative						MW (g/mol)	m/z			Linkage
	Chemical Shifts							δ of Connected	Inter residual connectivity		
5.29	1,3,5-Tri- <i>O</i> -acetyl-1-deuterio-2,4,6-tri- <i>O</i> -methyl-D-mannitol						351	87, 102, 129, 161, 202, 234			(1,3)
Linkage	H1	H2	H3	H4	H5	H6/H6'	H (δ ppm)	C (δ ppm)	NOESY (H/H)	HMBC (H/C)	
5.39	1,3,4,5-Tetra- <i>O</i> -acetyl-1-deuterio-2,6-di- <i>O</i> -methyl-D-mannitol						379	87, 101, 129, 161, 202, 262	139	A-H1/C-H6 A-H1/C-H6'	(1,3,4)
A											
β -D-Xylp-(1→	4.76	3.66	3.80	3.99	4.29/3.64	-	4.42/4.21	69	A-H1/C-H6 A-H1/C-H6'	(1,3,4)	
	104	76	63	70	65	379	87, 101, 129, 161, 202, 262	139	A-H1/C-H6 A-H1/C-H6'	(1,3,4)	
B											
β -D-Glcp-(1→	4.87	3.73	3.85	3.95	4.13	-	87, 115, 129, 157, 185, 260	178	B-H1/F-H2	(1,2,3,4)	
	102	70	70	70	70	407 175	87, 115, 129, 157, 185, 260	178	B-H1/F-H2	(1,2,3,4)	
C											
5.56	1,3,5,6-Tetra- <i>O</i> -acetyl-1-deuterio-2,4-di- <i>O</i> - \rightarrow 3,6)- α -D-Manp-(1→						379	87, 101, 118, 129, 160, 189, 234			(1,3,6)
	5.44	4.56	4.13	4.27	3.94	4.42/4.21	4.38	78	C-H1/G-H3	C-H1/G-C6	
	103	70	77	73	72	69	87, 101, 118, 129, 160, 189, 234	78	C-H1/G-H3	C-H1/G-C6	
D											
5.63	1,3,4,5,6-Penta- <i>O</i> -acetyl-1-deuterio-2- <i>O</i> -methyl-D-mannitol						407	118, 139			(1,3,4,6)
\rightarrow 3)- α -D-Manp-(→	5.46	4.56	4.29	4.04	3.93	4.11/4.24	4.43	77	D-H1/C-H3	D-H1/C-C3	
	103	70	79	66	72	61	4.43	77	D-H1/C-H3	D-H1/C-C3	
E											
5.69	1,2,3,5,6-Penta- <i>O</i> -acetyl-1-deuterio-4- <i>O</i> -methyl-D-mannitol						407	87, 129, 189, 162			(1,2,3,6)
\rightarrow 3)- α -D-Manp-(1→	5.52	4.59	4.35	4.12	4.38	4.23/4.15	4.29	79	E-H1/D-H3	E-H1/D-C3	
	102	70	70	70	73	61	4.29	79	E-H1/D-H3	E-H1/D-C3	
F											
5.78	1,2,3,4,5-Penta- <i>O</i> -acetyl-1-deuterio-D-xylitol						363	86, 115, 128, 145, 159, 188, 218			(1,2,3,4)
\rightarrow 2,3)- α -D-Manp-(1→	5.60	4.62	4.40	4.12	3.93	4.15/4.22	4.35	79	F-H1/E-H3	F-H1/E-C3	
	100	78	78	67	76	61	4.35	79	F-H1/E-H3	F-H1/E-C3	
G											
\rightarrow 6)- α -D-Manp-(1→	5.62	4.62	4.38	3.98	3.81	4.10/4.15	4.40	78	G-H1/F-H3	G-H1/F-C3	
	100	77	78	72	76	61	4.40	78	G-H1/F-H3	G-H1/F-C3	

Table S5. Hydrogen bonds between AAPS and the corresponding residue in dimeric TLR4/MD-2 complexes.

D	C ₂ -OAc	Side chain of R434 (mTLR4*)
E	C ₆ -OH	Backbone carbonyl group of N359 (mTLR4)
F	C ₄ -OAc C ₆ -OH C ₆ -OH	Side chain of Y102 (mMD-2) Side chain of E92 (mMD-2) Backbone amine group of V93 (mMD-2)
B	C ₂ -OH C ₄ -OH C ₅ -COOH C ₂ -OH C ₂ -OH	Side chain of R434 (mTLR4*) Side chain of R434 (mTLR4*) Side chain of S413 (mTLR4*) Side chain of E92 (mMD-2) Side chain of R90 (mMD-2)
A	C ₄ -OAc C ₆ -OH	Side chain of Y131 (mMD-2) Side chain of E92 (mMD-2)